Unfolding of Acrylodan-Labeled Human Serum Albumin Probed by Steady-State and Time-Resolved Fluorescence Methods

Kulwinder Flora,* John D. Brennan,* Gary A. Baker,# Meagan A. Doody,# and Frank V. Bright#
*Department of Chemistry, Brock University, St. Catharines, Ontario L2S 3A1, Canada, and #Department of Chemistry, Natural Sciences Complex, State University of New York at Buffalo, Buffalo, New York 14260-3000, USA

ABSTRACT Steady-state and time-resolved fluorescence spectroscopy was used to follow the local and global changes in structure and dynamics during chemical and thermal denaturation of unlabeled human serum albumin (HSA) and HSA with an acrylodan moiety bound to Cys^{34}. Acrylodan fluorescence was monitored to obtain information about unfolding processes in domain I, and the emission of the Trp residue at position 214 was used to examine domain II. In addition, Trp-to-acrylodan resonance energy transfer was examined to probe interdomain spatial relationships during unfolding. Increasing the temperature to less than 50°C or adding less than 1.0 M GdHCl resulted in an initial, reversible separation of domains I and II. Denaturation by heating to 70°C or by adding 2.0 M GdHCl resulted in irreversible unfolding of domain II. Further denaturation of HSA by either method resulted in irreversible unfolding of domain I. These results clearly demonstrate that HSA unfolds by a pathway involving at least three distinct steps. The low detection limits and high information content of dual probe fluorescence should allow this technique to be used to study the unfolding behavior of entrapped or immobilized HSA.

INTRODUCTION

Human serum albumin (HSA) is a large protein that is formed from a single polypeptide chain of 585 residues (Carter and Ho, 1994). The structure is divided into three major domains, and contains a total of 17 disulfide bonds (Brown, 1977). Despite the size and complexity of HSA, there is only a single Trp residue within the protein at position 214 in domain II (Carter and Ho, 1994). In addition, the protein contains only one free Cys residue at position 34 in domain I (Brown, 1977). The presence of the free thiol allows for site-specific labeling of the protein with chromophoric or fluorescent probes (Suzukida et al., 1983; Hagag et al., 1983; Ingersoll et al., 1996; Jordon et al., 1995; Wang et al., 1996; Narazaki et al, 1997; Lundgren et al., 1995).

HSA is the most abundant human blood protein and has the ability to bind several ligands, including small aromatic and heterocyclic carboxylic acids, such as the nonsteroidal antiinflammatory drugs (NSAIDs) (Sudlow et al., 1976). The ability of HSA to bind multiple ligands, combined with the size and complexity of the protein structure (which is in some ways reminiscent of enzymes and antibodies), has resulted in the protein becoming a popular model system for studies of immobilized or entrapped biorecognition elements that are employed in biosensor devices (Ingersoll et al., 1996; Jordon et al., 1995; Wang et al., 1996; Narazaki et al., 1997; Lundgren et al., 1995). Both unlabeled HSA and HSA labeled with the fluorescent probe acrylodan at Cys^{34} have been examined in solution and when immobilized to inorganic surfaces (Ingersoll et al., 1996; Jordon et al., 1995; Wang et al., 1996; Narazaki et al., 1997; Lundgren et al., 1995). The acrylodan probe was chosen for these studies because it is sensitive to the local environmental dipolarity and dynamics within the binding pocket surrounding Cys^{34} (Lundgren et al., 1995; Prendergast et al., 1983; Ilich and Prendergast, 1989; Clark and Burtnick, 1988; Yem et al., 1992). The acrylodan probe allowed the structure and dynamics of acrylodan-labeled HSA (HSA-Ac) to be examined, and allowed factors such as the accessibility of the reporter group to be monitored (Suzukida et al., 1983; Hagag et al., 1983; Ingersoll et al., 1996; Jordon et al., 1995).

One of the issues that is of interest for both free and immobilized proteins is the retention of protein function and how this relates to changes in the protein structure. This becomes especially important when one desires information on the effects of different encapsulation or immobilization protocols on protein structure and/or function. Several studies have appeared that have examined the structure, stability, and unfolding pathway of unlabeled HSA in solution (Pico, 1995, 1996, 1997; Wetzel et al., 1980; Tayyab et al., 1995; Lee and Hirose, 1992; Wallevik, 1973; Farruggia et al., 1997; Chmelik and Kalous, 1982). A variety of techniques have been applied, including NMR (Price et al., 1993), circular dichroism (Wetzel et al., 1980), differential scanning calorimetry (Pico, 1995, 1996, 1997), and measurement of intrinsic fluorescence (Pico, 1995; Farruggia et al., 1997). In addition, there is a recent report in which the steady-state and time-resolved fluorescence of the acrylodan label has been monitored during chemical denaturation of HSA-Ac in solution (Narazaki et al., 1997). Unfortunately, most of these techniques, with the exception of fluorescence spectroscopy, are not amenable to studies of entrapped or immobilized proteins. Furthermore, the information that is normally obtained from fluorescence studies

Received for publication 9 January 1998 and in final form 4 May 1998.

Address reprint requests to Dr. John D. Brennan, Department of Chemistry, Brock University, St. Catharines, ON L2S 3A1, Canada. Tel.: 905-688-5550, ext. 4115; Fax: 905-682-9020; E-mail: jbrennan@chemiris.labs.brocku.ca.

0006-3495/98/08/1084/13 $2.00

is often not sufficient to characterize subtle changes in the structure of large proteins. It is important to recognize that no studies have appeared that comprehensively describe the fluorescence behavior of both labeled and unlabelled HSA and how the fluorescence is affected by changes in structure and dynamics that are caused by thermally and chemically denaturing the protein.

In the present work, the emission of the acrylodan moiety attached at Cys^{34} is used to provide information on the local structure and dynamics of domain I, and the fluorescence of the single Trp residue is used to provide information on the local structure and dynamics of domain II during thermal and chemical denaturation. We report a detailed investigation of the steady-state fluorescence, steady-state anisotropy, and time-resolved fluorescence behavior of both Trp and acrylodan. Such studies provide a large amount of information, including local polarity, dynamics, and probe accessibility from two locations within the protein. In addition, we show here for the first time that the monitoring of Trp fluorescence from HSA-Ac provides the ability to investigate the spatial relationship between the Trp and acrylodan probes by resonance energy transfer techniques, owing to the overlap of the acrylodan excitation spectrum and the Trp emission spectrum. HSA has previously been labeled at the Cys residue for the purpose of examining interdomain spacings via energy transfer (Suzukida et al., 1983; Hagag et al., 1983). However, in this previous work only the effects of pH-induced structural alterations on the energy transfer efficiency were examined. Unfolding studies were not done with the labeled protein. In the present work, energy transfer measurements are used to provide a convenient method for examining changes in interdomain distances during denaturation and refolding, providing information on the spatial relationships between domains I and II.

The reversibility of unfolding at different stages and its correlation to protein function are also examined via binding of the fluorescent ligand salicylate (Brown and Crooks, 1976; Kerestes-Nagy et al., 1972; Hultmark et al., 1975). Salicylate binding studies provide information on the relationship between protein structure and function. By combining all of the fluorescence and binding data, we have been able to elucidate subtle features of the protein unfolding pathway that are not easily observed by other methods. These observations provide the key groundwork for future studies involving entrapped HSA and HSA-Ac.

MATERIALS AND METHODS

Materials

HSA (essentially fatty acid free), sodium salicylate, *N*-acetyltryptophanamide (NATA), and 3500 MW cutoff dialysis tubing were obtained from Sigma (St. Louis, MO). 6-Acryloyl-2-(dimethylamino)naphthalene (acrylodan) was obtained from Molecular Probes (Eugene, OR). 1,4-Bis(4-methyl-5-phenyl-2-oxazolyl)benzene (Me_2-POPOP), acrylamide (99+%), and sodium azide (99%) were supplied by Aldrich (Milwaukee, WI). The guanidine hydrochloride (GdHCl) (Sequanol grade) was from Pierce (Rockford, IL). The Sephadex G-25 fine powder was supplied by Pharmacia Biotech (Uppsala, Sweden). All water was distilled twice and deionized to a specific resistivity of at least 18 MΩ·cm with a Milli-Q 5 stage water purification system. All other chemicals were of analytical grade and were used without further purification.

Protein labeling and purification

A small amount of protein (1 mg) was dissolved into 1 ml of 10 mM phosphate buffer containing 100 mM KCl at pH 7.2. This was then passed through a Sephadex G-25 column (height 10–20 cm, diameter 1 cm) with 10 mM phosphate buffer to elute the protein. The purified protein was labeled as described previously (Wang et al., 1996). Briefly, acrylodan and HSA were mixed in a 2:1 molar ratio and allowed to stir in the dark for 24 h at room temperature. Unlabelled acrylodan was dialyzed against 10 mM phosphate buffer over a 4-day period, with an exchange of buffer every 12 h. The labeled protein was then passed through a G-25 sephadex column to dislodge any unreacted label. The concentration of labeled protein was found by using $\epsilon_{278} = 8{,}700\ M^{-1}\ cm^{-1}$ and $\epsilon_{365} = 12{,}800\ M^{-1}\ cm^{-1}$ for acrylodan (Edmiston et al., 1994) and $\epsilon_{277} = 36{,}000\ M^{-1}\ cm^{-1}$ for HSA (Pico, 1997). The labeling efficiency was determined to be >80%.

Steady-state fluorescence measurements

Fluorescence excitation and emission spectra were collected from labeled and unlabeled HSA with instrumentation that has been described previously (Zheng et al., 1997). Samples containing unlabeled HSA were excited at 295 nm, and emission was collected from 305 nm to 450 nm in 1-nm increments with an integration time of 0.50 s, using 4 nm bandpasses in both the excitation and emission paths. Acrylodan-labeled HSA was excited at 360 nm, with emission collected from 400 nm to 600 nm to examine the acrylodan residue alone. For energy transfer experiments, the labeled protein was excited at 295 nm, and emission was collected from 305 nm to 600 nm. Excitation spectra of acrylodan were collected from 315 nm to 470 nm with emission at 500 nm.

Steady-state fluorescence anisotropy measurements were done as described elsewhere (Wang and Bright, 1993), with excitation at 295 nm and emission at 340 nm for studies of Trp, 360 nm excitation and 500 nm emission to measure the anisotropy of acrylodan, or 295 nm excitation and 500 nm emission to measure the effects of energy transfer on anisotropy. All experiments were done with 30 μM protein to provide a sufficient signal with the polarizers in place. Steady-state anisotropy values (r) were used to obtain average rotational correlation times (ϕ), using the mean fluorescence lifetime (τ) and limiting anisotropy (r_0), as follows:

$$r = \frac{r_0}{1 + (\tau/\phi)} \tag{1}$$

Time-resolved fluorescence measurements

Time-resolved fluorescence measurements of Trp were performed by the time-correlated single photon counting method (O'Connor and Phillips, 1984). The excitation source was a cavity dumped dye laser synchronously pumped by an actively mode-locked argon ion laser (Spectra Physics) operating at 825 kHz with a pulse width of 15 ps. Emission, following vertically polarized excitation at 295 nm, was detected (right angle geometry) after passing through a polarizer set at 55° to the vertical and a JY H10 monochromator with a 4-nm bandpass, using a Hamamatsu 1564U-01 microchannel plate photomultiplier tube. The channel width was 10 ps/channel, and data were collected in 1024 channels. The instrument response function was determined from the Raman scattering of water and typically had a FWHM of ~70 ps. Counts from a blank were measured for each sample for the same accumulation time, and the blank counts were subtracted from the sample decay curve.

Time-resolved intensity and anisotropy decay data for the acrylodan label were acquired in the frequency domain with a SLM 48000 MHF multifrequency phase-modulation fluorometer. An argon ion laser (Coherent, model Innova 90-6) operating at 351.1 nm was used as the excitation source. A bandpass filter was placed in the excitation path to minimize extraneous plasma discharge in the detection system. Magic angle polarization was used for all excited-state intensity decay experiments. Me_2POPOP in ethanol served as the reference lifetime standard; its lifetime was assigned a value of 1.45 ns. For all experiments, the Pockel cell was operated at a repetition rate of 5 MHz. Typically, data were collected for 60–90 s over a frequency range of 5–250 MHz. All multifrequency phase and modulation data were analyzed according to a global analysis method described elsewhere (Wang and Bright, 1993).

For both time-domain and frequency-domain measurements of intensity decays, the function describing the fluorescence intensity decay was assumed to be a sum of exponential components:

$$I(\lambda, t) = \sum_i \alpha_i(\lambda)\exp(-t/\tau_i) \tag{2}$$

where τ_i is the decay time of the ith component and $\alpha_i(\lambda)$ is the preexponential factor at emission wavelength λ. The fractional fluorescence of component i at wavelength λ ($f_i(\lambda)$) was calculated from

$$f_i(\lambda) = \left(\alpha_i(\lambda)\tau_i \Big/ \sum_i \alpha_i(\lambda)\tau_i\right) \tag{3}$$

From this, the mean lifetime values are obtained from the following equation:

$$\langle\tau\rangle = \sum_i f_i\tau_i \tag{4}$$

Time-resolved decays of fluorescence anisotropy ($r(t)$) were fit to a double exponential decay of the form

$$r(t) = r_0[\beta_1 \exp(-t/\phi_1) + \beta_2 \exp(-t/\phi_2)] \tag{5}$$

where ϕ_1 depends solely on the local rotational reorientation of the probe and ϕ_2 depends on the global motions of the entire biomolecule. The terms β_1 and β_2 represent the fractional contributions to the total anisotropy decay from the local and global motions, respectively ($\Sigma\beta_i = 1$). In the situation where the local probe motion is faster than the global motion of the entire protein, the local rotational motion of the probe ϕ_L is given as $1/(1/\phi_2 + 1/\phi_1)$.

A semiangle (θ) can be associated with the cone within which the probe is able to precess during its excited-state fluorescence lifetime, given by

$$\theta = \cos^{-1}[0.5(8(\beta_1)^{1/2} + 1)^{1/2} - 1] \tag{6}$$

If the environment surrounding the probe is totally restrictive to the local probe motion, θ will approach 0°. In contrast, complete freedom of the probe to rotationally reorient will result in a θ value of 90°. Intermediate θ values reflect partial freedom of the probe to reorient within its cybotactic region.

Energy transfer measurements

The efficiency of energy transfer (E) as a function of distance (R) between two probes was determined from fluorescence lifetime values as follows (Campbell and Dwek, 1984):

$$E = \left(1 - \frac{\Phi_{DA}}{\Phi_D}\right) = \left(1 - \frac{\tau_{DA}}{\tau_D}\right) = \frac{R_0^6}{R^6 + R_0^6} \tag{7}$$

where R_0 represents the distance at which energy transfer is 50% efficient, Φ_{DA} and τ_{DA} are the quantum yield and fluorescence lifetime of the donor in the presence of the acceptor, respectively, and Φ_D and τ_D are the unquenched donor quantum yield and lifetime in the absence of acceptor, respectively. The value of R_0 (in nanometers) was obtained from Eq. 8 (Campbell and Dwek, 1984):

$$R_0 = 9.79 \times 10^2(Jn^{-4}\kappa^2\Phi_D)^{1/6} \tag{8}$$

where J is the overlap integral, n is the solution refractive index, and κ^2 is the orientation factor between the donor and acceptor electronic transition dipole moments. The overlap integral was determined by using the overlap of the acrylodan excitation spectrum and the Trp emission spectrum, according to standard methods (Campbell and Dwek, 1984).

Chemical denaturation studies

Chemical denaturation studies were carried out with 1.50 ml of 0.5 μM HSA or 1.0 μM HSA-Ac solution. Samples were titrated with 8.0 M GdHCl with constant stirring, and a minimum of 10 min was allowed for equilibration (with a shutter blocking the excitation light). A fluorescence spectrum or a steady-state anisotropy value was collected at each point for both the sample and a blank containing an identical concentration of GdHCl. The spectra were corrected for contributions from the blank and instrument factors as well as for dilution factors. Unfolding curves were obtained by integrating and normalizing the spectra and were fit by using Eq. 9 (Santoro and Bolen, 1988):

$$F_D = \frac{(F_N + m_N[D]) + (F_U + m_U[D]\exp\{-\Delta G_{(F\rightarrow U)}/RT + m_G[D]/RT\}}{1 + \exp[-(\Delta G_{(F\rightarrow U)}/RT + m_G[D]/RT)]} \tag{9}$$

where F_D is the value of the fluorescence intensity (or anisotropy) at a given concentration of denaturant, [D], R is the gas constant, and T is the temperature. The remaining six terms are fitting parameters, where F_N and F_U are the values of the intensity or anisotropy extrapolated to zero denaturant concentration for the native and unfolded states, respectively; m_N and m_U are the slopes for the dependencies of F_N and F_U on denaturant concentration; $\Delta G_{(F\rightarrow U)}$ is the free energy of unfolding; and m_G is the slope describing the dependence of $\Delta G_{(F\rightarrow U)}$ on denaturant concentration. The transition midpoint ($D_{1/2}$) values can be calculated by dividing $\Delta G_{(F\rightarrow U)}$ by $-m_G$.

Thermal denaturation studies

A volume of 1.5 ml of 1.0 μM HSA or HSA-Ac was placed in a quartz fluorimeter cuvette. The temperature was raised in ~3°C increments, starting at 20°C and going to 70°C or 80°C. A fluorescence spectrum or anisotropy value was collected from the sample and from an appropriate blank at each temperature. The temperature of the solution in the cuvette was measured directly with a thermistor probe (Hanna Instruments model 9043A) to account for loss of heat through the Tygon tubing connecting the sample holder and the water bath. The samples were allowed to equilibrate for at least 5 min at each temperature before readings were taken with a shutter blocking the excitation beam. The spectra were integrated over a 40-nm window centered about the emission maximum. The resulting unfolding curve was analyzed by nonlinear fitting to the equation described by Eftink (1994):

$$F_T = \frac{F_{0N} + s_N T + [F_{0U} + s_U T]\exp\{[-\Delta H^0_{un} + T\Delta S^0_{un}]/RT\}}{1 + \exp\{-[\Delta H^0_{un} + T\Delta S^0_{un}]/RT\}} \tag{10}$$

where F_T is the measured intensity (or anisotropy) at some temperature T, and R is the gas constant. The remaining six terms are fitting parameters, where F_{0N} and F_{0U} are the fluorescence intensity (or anisotropy) of the native and unfolded states, respectively; s_N and s_U are the baseline slopes of the native and unfolded states as a function of temperature, respectively; and ΔH°_{un} and ΔS°_{un} are the enthalpy change and entropy change for the

unfolding reaction, respectively. The free energy change for unfolding (ΔG_{un}) is then determined by

$$\Delta G_{un}(T_r) = \Delta H^0_{un} - T_r \Delta S^0_{un} + \Delta C_{p,un}[(T_r - T_{un}) - T_{un} \ln(T_r/T_{un})] \quad (11)$$

where T_r is a reference temperature (usually 20°C), T_{un} is the temperature of unfolding (given by $\Delta H^\circ_{un}/\Delta S^\circ_{un}$), and $\Delta C_{p,un}$ is the differential heat capacity for unfolding, which accounts for the temperature sensitivity of the entropy and enthalpy terms on going from T_r to T_{un}.

Salicylate titrations of HSA

A solution of 5 μM HSA in 10 mM phosphate buffer was titrated with 50 μM salicylate in 10 mM phosphate buffer at pH 7.2. Spectra were collected for salicylate in both the presence and absence of HSA. A 40-nm window centered about the emission wavelength maximum at 408 nm was integrated to provide intensity values for the ligand at each salicylate concentration, and this value was corrected for dilution factors and for the fluorescence of the blank. Linear regression was performed on the ligand binding curve to quantitate the relative binding affinity of the HSA (Brown and Crooks, 1976). This experiment was performed on native, thermally denatured, and chemically denatured protein samples.

Acrylamide quenching studies

Acrylamide was used to quench the Trp residue in unlabeled HSA. A volume of 2.0 ml of a 0.5 μM HSA solution was titrated with 8.0 M acrylamide in buffer. A fluorescence spectrum was collected from the sample and an appropriate blank after each addition with excitation at 295 nm and emission from 305 nm to 450 nm. Spectra were corrected for sample dilution and were integrated from 310 nm to 450 nm. The quenching data were fit using a modified version of the Stern-Volmer equation, which accounted for both dynamic and static contributions to the quenching process:

$$\frac{F_0}{Fe^{V[Q]}} = 1 + K_{SV}[Q] = 1 + k_q \tau_0 [Q] \quad (12)$$

where F_0 is the fluorescence intensity in the absence of quencher, F is the fluorescence in the presence of quencher, [Q] is the molar concentration of the quencher, K_{SV} is the Stern-Volmer quenching constant for the collisional process (M^{-1}), k_q is the bimolecular quenching constant ($M^{-1} \cdot s^{-1}$), τ_0 is the unquenched excited state fluorescence lifetime, and V is the active volume of the sphere surrounding the fluorophore, within which no diffusion is necessary to initiate quenching (Eftink and Ghiron, 1976).

O_2 quenching of HSA-Ac

The oxygen quenching of the acrylodan residue of HSA-Ac was carried out with a stainless steel high-pressure O_2 cell similar to the one described by Lakowicz et al. (Lakowicz and Weber, 1973) (Note: These experiments require the use of moderately high pressures. One must exercise extreme caution when working with high-pressure gases, especially O_2.) A temperature-regulated fluid was pumped directly through a coil within the cell to ensure temperature control (20 ± 1°C). O_2 from a standard gas cylinder was introduced directly into the cell through stainless steel tubing and a valve. The internal cell pressure was monitored (±1 psia) with a standard digital pressure transducer. The solution was constantly stirred throughout the experiment, and all samples were allowed to equilibrate until the fluorescence was constant (Ingersoll et al., 1996). The concentration of HSA-Ac within the cell was 2.0 μM. Data were analyzed according to a protocol outlined elsewhere (Ingersoll et al., 1996).

RESULTS AND DISCUSSION

Chemical denaturation

The unfolding behavior of HSA and HSA-Ac was first examined by chemical denaturation with GdHCl. The changes in the steady-state and time-resolved fluorescence intensity and anisotropy were monitored for both the Trp in HSA and HSA-Ac and for the acrylodan moiety of HSA-Ac. The Trp residue within the native, unlabeled protein had an emission maximum of 335 nm, a quantum yield of 0.14 ± 0.01, and a steady-state anisotropy value of 0.180 ± 0.002. From Eq. 1, this indicates that the average rotational correlation time for native HSA is 4.15 ± 0.04 ns. These values are consistent with the Trp residue being located in an environment of intermediate polarity with an intermediate degree of motion (i.e., some local motion that reduces r).

Denaturation of HSA using GdHCl was monitored by changes in integrated fluorescence intensity and steady-state anisotropy, as shown in Figs. 1 *A* and 2. Initially, there was a preunfolding baseline with no major changes in intensity or anisotropy. However, there was a slight blue shift in the emission wavelength of the Trp residue (to a value of 330 nm) before the first stage of unfolding (spectra not shown). The intensity data, shown in Fig. 1 *A*, indicated that the protein denatured by a two-stage process. The first unfolding transition occurred between 1.0 M and 2.2 M with a large change in intensity (50%). This transition was accompanied by a red shift in the wavelength from 330 nm to 345 nm. The intensity data also indicated that there was a second unfolding transition between 2.2 M and 3.0 M, with a much smaller change in intensity (~20%), and no further wavelength shift. Anisotropy changes, shown in Fig. 2 (*lower curve*), showed one distinct unfolding step at a denaturant level similar to that observed for intensity measurements, and a drawn-out baseline, which is presumably due to the second unfolding step. The final anisotropy value was 0.070 ± 0.002 at 4.0 M GdHCl, corresponding to an average rotational correlation time of 0.58 ± 0.02 ns. The decrease in anisotropy is indicative of a substantial increase in the mobility of the Trp residue, and is consistent with unfolding of the protein. The transition reported by steady-state fluorescence anisotropy measurements was broader than that reported by intensity measurements, consistent with the differential quantum yield weighting of the folded and unfolded forms of the protein (Eftink, 1994).

Acrylamide quenching of the Trp residue at different levels of GdHCl indicated that the value of k_q increased from 0.6×10^9 to 1.1×10^9 M^{-1} s^{-1} on going from 0.0 M to 2.0 M GdHCl. The results are consistent with the unfolding of domain II causing increased exposure of the Trp residue, and correspond to the range for the major emission wavelength shift. Beyond 2.0 M the k_q value remained constant at 1.0×10^9 M^{-1} s^{-1}, indicating that the second unfolding step did not cause changes in the exposure of the Trp residue. From this data, it appears that the unfolding of domain II occurs over the denaturant range between 1.0 and

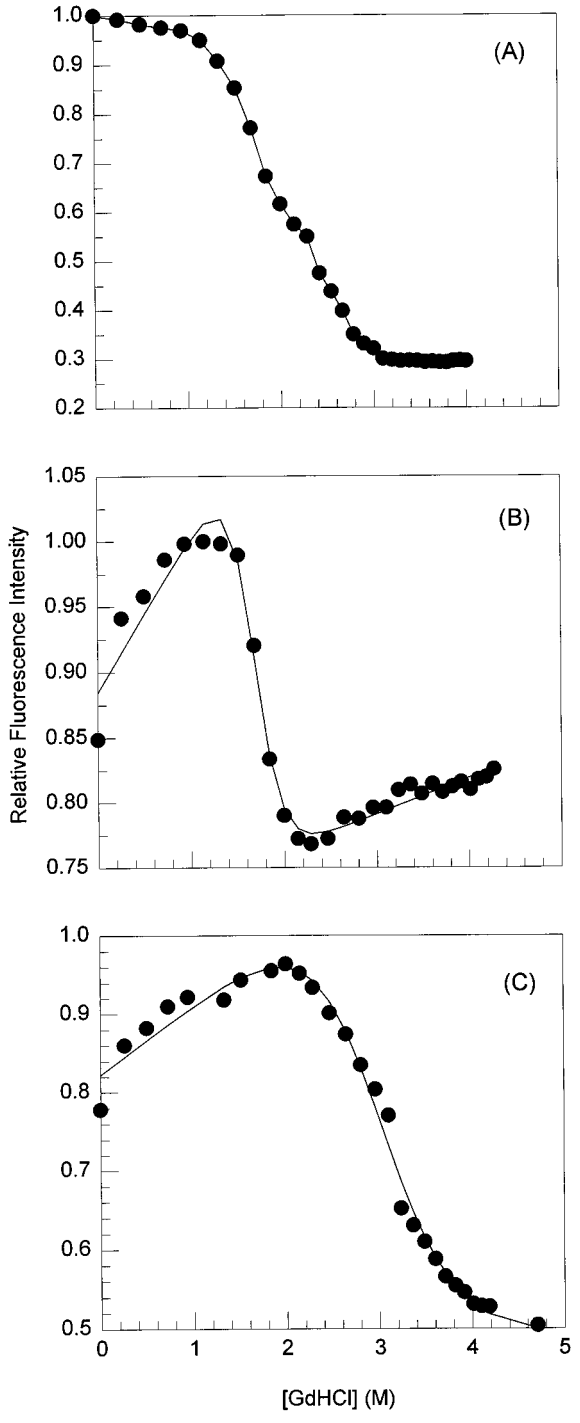

FIGURE 1 Changes in integrated intensity during chemical denaturation of HSA and HSA-Ac using GdHCl. (*A*) Trp emission from HSA excited at 295 nm. (*B*) Trp emission from HSA-Ac excited at 295 nm. (*C*) Acrylodan emission from HSA-Ac excited at 360 nm.

2.0 M, and a second unfolding step not directly involving domain II occurs at denaturant levels above 2.0 M.

Analysis of the unfolding curve (Fig. 1 *A*) by Eq. 9 provided $\Delta G_{(F\rightarrow U)}$ values of 30.0 ± 1.3 kJ · mol^{-1} for the first stage of unfolding and 35.0 ± 1.5 kJ · mol^{-1} for the second stage of unfolding, as shown in Table 1. Thus the

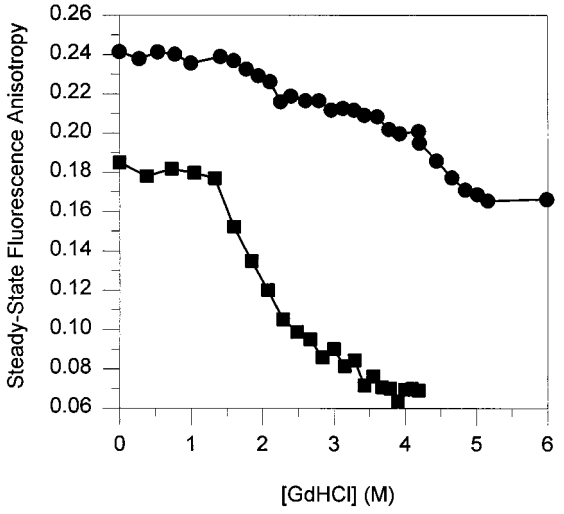

FIGURE 2 Steady-state anisotropy of HSA and HSA-Ac during chemical denaturation. ■, Anisotropy of Trp from HSA with excitation at 295 nm. ●, Anisotropy of acrylodan within HSA-Ac with excitation at 360 nm.

total change in free energy for unfolding of HSA was 65.0 ± 4.8 kJ · mol^{-1}. Farruggia et al. (1997) obtained a value of 23 kJ · mol^{-1} with a $D_{1/2}$ of 2.75 M for unfolding of HSA, but did not witness a two-stage unfolding process. Our initial experimental results indicated a one-step unfolding with a $\Delta G_{(F\rightarrow U)}$ value of 25.9 ± 2.2 kJ · mol^{-1}, but these results were obtained under conditions where samples were not given sufficient time to reach equilibrium after the addition of GdHCl. Only when sufficiently long equilibration times were used (10 min per aliquot of denaturant) was the unfolding of HSA observed to be a multistep process.

Removal of GdHCl by dialysis resulted in a recovery of the shape of the spectral contour for Trp, along with recovery in terms of emission wavelength, anisotropy, and quencher accessibility. However, the intensity did not recover to the initial value before unfolding, suggesting that the native structure may not have been fully recovered. To further examine the changes in protein structure and function on denaturation and recovery, we determined the binding of salicylate to HSA at different denaturant levels and for protein that had the GdHCl removed by dialysis. HSA containing even low levels of GdHCl (less than 1.0 M) was unable to bind salicylate. However, at such levels the removal of the denaturant by dialysis restored the binding capability of the protein, indicating that the initial conformational changes reported by the blue shift in the Trp emission wavelength were reversible. Denaturation and recovery of HSA, using GdHCl at levels of 2.0 M or higher, where domain II was fully unfolded, resulted in a large decrease in the ability of the protein to bind salicylate, showing that domain II unfolding was not fully reversible. Thus, even though the spectral and quenching data suggest a similar environment for the Trp residue for native and refolded HSA, the binding studies clearly show that unfolding of domain II causes irreversible changes in the structure and function of the protein.

TABLE 1 Thermodynamic parameters for GdHCl-induced unfolding of HSA

Sample	$\Delta G_{(F\rightarrow U)}$ (kJ · mol^{-1})*	$-m_G$ (kJ · L · mol^{-2})*	$D_{1/2}$ (M)#	χ^{2}§
Trp in HSA (Stage 1)¶	30.0 ± 1.8	20.1 ± 1.1	1.5 ± 0.2	0.97
Stage 2‖	35.0 ± 1.5	13.0 ± 0.9	2.7 ± 0.2	0.97
Trp in HSA-Ac**	29.7 ± 5.0	15.0 ± 2.4	2.0 ± 0.2	0.98
Acrylodan in HSA-Ac##	14.7 ± 1.1	5.7 ± 0.5	2.6 ± 0.3	0.99

*These values were obtained by fitting of unfolding curves to Eq. 3.
#This value was obtained by dividing ΔG_{un} by $-m_G$.
§Determined from nonlinear curve fitting, using SigmaPlot 1.02 for Windows.
¶Fitting parameters: $F_N = 0.999$, $F_U = 1.104$, $m_N = -0.033$, $m_U = -0.245$.
‖Fitting parameters: $F_N = 1.044$, $F_U = 0.332$, $m_N = -0.245$, $m_U = -0.011$.
**Fitting parameters: $F_N = 0.942$, $F_U = 0.632$, $m_N = 0.050$, $m_U = 0.016$.
##Fitting parameters: $F_N = 0.862$, $F_U = 0.832$, $m_N = 0.093$, $m_U = -0.046$.

To examine the unfolding behavior of domain I, denaturation of HSA-Ac was carried out. Incorporation of the acrylodan label resulted in dramatic changes in the intensity of the Trp signal for both the native and the unfolded protein, although the spectral contours corresponding to these forms (i.e., emission maximum and full width at half-maximum) were identical to those obtained for the unlabeled protein (spectra not shown). The measured quantum yield of the native protein dropped from 0.14 ± 0.01 to 0.03 ± 0.01, indicating that acrylodan was able to quench the Trp fluorescence. These results strongly suggest that the acrylodan label influenced the Trp signal, owing to a resonance energy transfer effect, with the Trp residue acting as the donor and the acrylodan label acting as the acceptor. This effect is described in more detail below.

Chemical denaturation of HSA-Ac resulted in a significantly different unfolding curve when the Trp emission was monitored, as shown in Fig. 1 *B*. The unfolding curve for the protein was altered such that the intensity of the Trp signal increased significantly (15%) between 0.0 M and 1.0 M denaturant. This range is similar to that for the blue shift in the Trp emission wavelength maximum, and is consistent with a separation of domain I and domain II such that the quenching of the Trp residue is partially relieved. The main unfolding transition occurred between 1.0 M and 2.0 M of GdHCl, and had a $D_{1/2}$ value of 2.0 M, which was similar to that obtained for the unfolding of unlabeled HSA. Beyond 2.0 M the intensity of the Trp emission increased in a fairly linear fashion, suggesting that the unfolding of domain I containing the acrylodan label was affecting the Trp signal from domain II, in agreement with the behavior observed for unlabeled HSA (Fig. 1 *A*). It is interesting to note that the second unfolding step is not observable, unlike the case of unlabeled HSA. This is likely due to a broad distribution of Trp-acrylodan donor-acceptor distances within the partially denatured HSA-Ac, causing a broadening of the unfolding transition.

Unfolding curves were also obtained for HSA-Ac when the acrylodan label was excited directly at 360 nm and the acrylodan emission was observed during denaturation. Fig. 1 *C* shows the changes in integrated intensity during denaturation, and Fig. 2 (*upper curve*) shows the changes in steady-state anisotropy. O_2 quenching of the acrylodan label was also carried out at various denaturant levels. In this case, the intensity of the acrylodan label increased by ~15% during the addition of the first 2.0 M of denaturant, reaching a maximum between 1.5 and 2.0 M GdHCl, although the anisotropy and k_q value remained relatively constant over this range. This range correlates to that for the initial domain separation and unfolding of domain II, as shown by the Trp fluorescence of HSA and HSA-Ac, and indicates that these processes result in a change in the local conformation of domain I in the region surrounding Cys^{34}. The main unfolding transition reported by the acrylodan intensity changes occurred over a fairly broad range between 2.0 M and 4.0 M GdHCl, with a $D_{1/2}$ value of 2.7 M. The k_q value also increased by nearly twofold over this range, indicating that the acrylodan moiety became more solvent exposed. Beyond 4.0 M GdHCl, the intensity and k_q value remained relatively constant, indicating that full unfolding of the structure occurred upon the addition of ~4.0 M GdHCl. The corresponding anisotropy decrease for the acrylodan label occurs in two stages, with a small anisotropy change between 1.0 M and 2.2 M denaturant, and a larger change between 4.0 and 5.0 M GdHCl. The initial change is consistent with an overall increase in the global motion of the protein upon unfolding of domain II. The second step is consistent with the unfolding of domain I. The steady-state anisotropy changes again lag behind the integrated intensity changes, as observed for Trp, owing to the differential quantum yield weighting of the native and unfolded states (Eftink, 1994). Overall, the results from the acrylodan emission clearly show that the unfolding of domain I occurs only after domain II has fully unfolded, and supports the presence of a multistep unfolding process, as suggested by changes in the Trp fluorescence of HSA.

The multistep unfolding profile reported by the intensity and anisotropy data provides evidence that the protein unfolding pathway involves at least one intermediate. This is contrary to the findings of Tayyab et al. (1995), who examined urea-induced denaturation of HSA with fluorescence measurements and found that unfolding apparently occurred in a single, concerted step. However, studies by Wallevick (1973) suggested that the unfolding of HSA with GdHCl is

a multistep process at physiological pH values, in agreement with our findings. Chmelik et al. (Chmelik and Kalous, 1982) have also reported finding, by polarography, a two-step unfolding of HSA by urea.

Time-resolved intensity data for the Trp residue within HSA and for the Trp and acrylodan within HSA-Ac were obtained for proteins in the presence of 0 M, 1.0 M, 2.0 M, and 4.0 M GdHCl, as shown in Table 2. The mean lifetime value for Trp in native HSA was 5.28 ± 0.03 ns, which is in reasonable agreement with the value of 5.60 ns reported elsewhere (Helms et al., 1997). Comparison of Trp lifetime values for HSA and HSA-Ac allowed for an examination, using Eq. 7, of interdomain distance relationships at different denaturant levels. The value of R_0 for the native protein was first calculated (and was determined to be 2.70 ± 0.03 nm) using a donor quantum yield of 0.14, a J value of $(8.91 \pm 0.09) \times 10^{-15}$ cm^3 M^{-1}, and with κ^2 set to 2/3 and n set to 1.50. Based on the differences in the intensity-weighted mean lifetime of native HSA and HSA-Ac, the energy transfer efficiency of the folded protein was determined to be 28.3 ± 0.2%, corresponding to an interdomain distance of 3.15 ± 0.03 nm. This value is in excellent agreement with the value of 3.18 nm reported by Hagag et al. (1983). At 1.0 M, the mean lifetime values of the Trp residue in HSA and HSA-Ac both dropped slightly, indicating a slight decrease in energy transfer efficiency to 25.0 ± 0.2%. This indicates that the interdomain distance had increased to 3.26 ± 0.03 nm, suggesting that interdomain separation likely occurred before domain unfolding took place. This interpretation is in agreement with the increase in Trp emission intensity observed during the initial stages of denaturation for HSA-Ac (Fig. 1 *B*).

At 2.0 M GdHCl, the mean lifetime value of Trp in both proteins dropped significantly, indicating a large change in the environment of the Trp residue. Comparison of the lifetime values for the two proteins indicated that the energy transfer efficiency increased to 36.7 ± 0.4%, corresponding to a decrease in the Trp-acrylodan distance to 2.96 ± 0.03 nm. This decrease in the donor-acceptor distance occurs at a point where domain II is unfolded but domain I is intact. Thus, under these conditions, the Trp residue is apparently free to move closer to the acrylodan moiety, producing a slight decrease in the average Trp-acrylodan distance. The overall structural change in the protein may explain the observed increase in the directly excited acrylodan emission intensity between 0.0 and 2.0 M GdHCl, shown in Fig. 2 *C*.

At 4.0 M GdHCl, the mean lifetime values of the Trp within HSA and HSA-Ac show a further decrease, and the fractional contribution of each decay component shifts to emphasize the two longer decay components. The energy transfer efficiency drops to 13.2 ± 0.1%, corresponding to an average Trp-acrylodan distance of 3.69 ± 0.05 nm. Thus, after domain I unfolds, the protein adopts an extended conformation, with the distance between the Trp and acrylodan moieties increasing substantially. The relative closeness of the two probes for the unfolded protein may be explained by the fact that the disulfides were not reduced; thus complete unfolding does not occur.

TABLE 2 Fluorescence intensity decay parameters for the Trp residue within HSA and HSA-Ac as a function of denaturant concentration

Sample	α_1	α_2	α_3	f_1*	f_2	f_3	τ_1 (ns)	τ_2 (ns)	τ_3 (ns)	$\langle\tau\rangle$ (ns)#	χ^2
Tryptophan in HSA											
0 M GdHCl	0.57	0.29	0.14	0.79	0.20	0.01	5.913	3.046	0.231	5.28	1.054
1 M GdHCl	0.59	0.24	0.17	0.85	0.14	0.01	5.453	2.135	0.080	4.98	1.103
2 M GdHCl	0.38	0.37	0.25	0.73	0.25	0.02	5.114	1.857	0.214	4.19	1.062
4 M GdHCl	0.48	0.41	0.11	0.70	0.28	0.02	3.230	1.516	0.310	2.73	1.004
0 M GdHCl (recovered)	0.40	0.35	0.25	0.73	0.25	0.02	5.951	2.251	0.257	4.92	1.089
Tryptophan in HSA-Ac											
0 M GdHCl	0.36	0.27	0.37	0.79	0.19	0.02	4.473	1.420	0.143	3.79	1.070
1 M GdHCl	0.31	0.29	0.40	0.77	0.21	0.02	4.439	1.325	0.074	3.70	1.010
2 M GdHCl	0.30	0.35	0.25	0.73	0.24	0.03	3.314	0.930	0.152	2.65	1.011
4 M GdHCl	0.22	0.35	0.42	0.61	0.34	0.05	3.229	1.118	0.147	2.36	1.020
Acrylodan in HSA-Ac											
0 M GdHCl	0.60	0.40	—	0.77	0.23	—	4.330	1.886	—	3.775	1.005
0.5 M GdHCl	0.61	0.39	—	0.80	0.20	—	4.212	1.656	—	3.698	1.017
1 M GdHCl	0.65	0.35	—	0.85	0.15	—	4.002	1.325	—	3.606	1.021
2 M GdHCl	0.65	0.35	—	0.84	0.16	—	3.972	1.377	—	3.562	1.009
4 M GdHCl	0.62	0.38	—	0.83	0.17	—	3.779	1.282	—	3.365	1.029
5 M GdHCl	0.61	0.39	—	0.81	0.19	—	3.610	1.312	—	3.166	1.045
6 M GdHCl	0.48	0.52	—	0.71	0.29	—	3.470	1.320	—	2.853	1.121

*Calculated from Eq. 3.
#Calculated from Eq. 4.

Refolding the protein by dialysis of the GdHCl resulted in the lifetime recovering to a value of 4.92 ± 0.04 ns. However, the fractional contribution of each decay component was different from those observed for the native protein. The results clearly indicated that the native structure was not recovered upon protein refolding, at least in the region of the Trp residue. The decay of Trp fluorescence intensity for refolded HSA-Ac could not be reliably fit, and therefore it was not possible to obtain Trp-acrylodan distance information in this case.

Time-resolved intensity measurements were also made of acrylodan within HSA-Ac, as a function of GdHCl concentration. The results are shown in Table 2. Both the long and short lifetime components decrease as the GdHCl concentration increases, as expected based on the unfolding model proposed above for HSA. The initial changes seen between 0.5 and 1.0 M GdHCl are consistent with changes in the local environment of the probe, whereas changes of the global protein structure are observed between 1.0 and 6.0 M GdHCl. These results support the suggestion that the major changes in the environment of the acrylodan label occur at higher levels of denaturant, which is consistent with the unfolding of domain I containing the acrylodan label at high denaturant levels.

Time-resolved fluorescence anisotropy decays of the acrylodan moiety in HSA-Ac were also measured. These results are summarized in Fig. 3. The results show that the initial global reorientation time is quite large (~80 ns), suggesting that multimers of the protein may have been present. A small decrease in the global rotational reorientation time occurs between 1.0 M and 3.0 M, suggesting that the global motion of the entire protein increases over this range of denaturant. There is also a small increase in the fractional contribution of the shorter rotational correlation time, suggesting greater acrylodan residue freedom. Between 3.0 M and 6.0 M GdHCl, the two rotational correlation times remain essentially constant; however, the contribution from the shorter component and the semiangle of rotation for the acrylodan label increase significantly. This is consistent with an opening of the pocket hosting the acrylodan reporter group, such that a higher proportion of acrylodan labels are able to freely rotate, and reflects the unfolding of domain 1 beyond 2.0 M GdHCl.

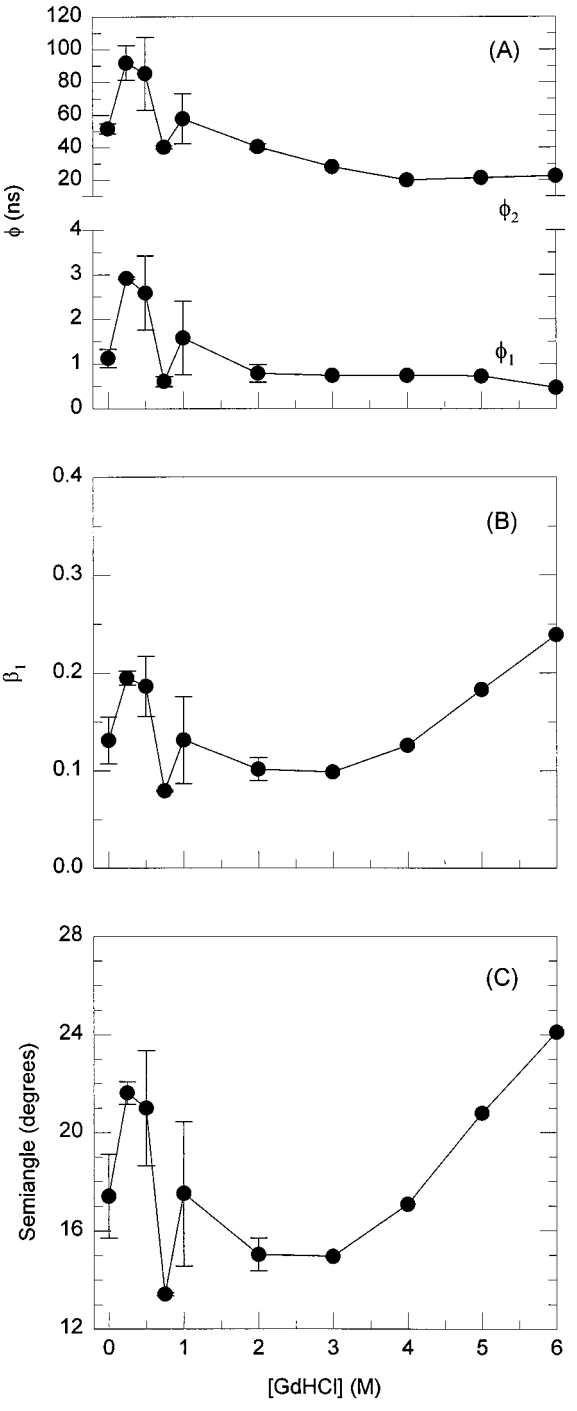

FIGURE 3 Time-resolved decay of acrylodan anisotropy during chemical denaturation of HSA-Ac. (*A*) Fluorescence rotational correlation times for global (ϕ_2) and local (ϕ_1) rotational components. (*B*) Fractional contribution of ϕ_1 as a function of denaturant concentration. (*C*) Semiangle of probe rotation obtained during chemical denaturation of the protein. The error bars on each panel denote ±1 standard deviation from at least three discrete measurements.

Thermal denaturation

Thermal denaturation experiments were also performed and were used to validate the multi-step unfolding model. Figs. 4 and 5 present the changes in integrated intensity and steady-state anisotropy as a function of temperature for HSA, HSA-Ac excited at 295 nm (Trp emission, not shown in Fig. 5), and HSA-Ac excited at 360 nm (acrylodan emission). Unfolding of HSA (*circles* in Fig. 4) appeared to occur as a single step, contrary to the results obtained for chemical denaturation of HSA as monitored by Trp intensity. The Trp intensity decreased by 60%, with the emission wavelength maximum blue shifting and the anisotropy decreasing from 0.180 ± 0.003 to 0.118 ± 0.002 during the unfolding transition. The latter anisotropy value corresponds to an average rotational correlation time of 1.25 ±

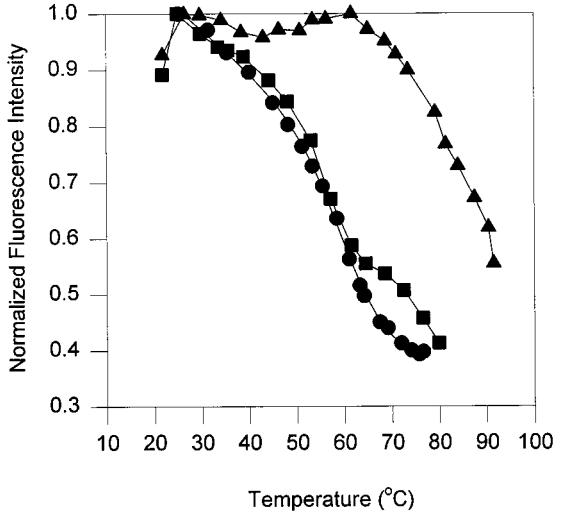

FIGURE 4 Changes in integrated intensity and emission wavelength of HSA and HSA-Ac monitored as a function of temperature. ●, Trp emission of HSA. ■, Trp emission from HSA-Ac. ▲, Acrylodan emission from HSA-Ac.

0.02 ns, which is double that obtained during chemical denaturation. Furthermore, above 60°C, the anisotropy of the Trp residue increased. Taken together, these results provide evidence that protein aggregates on thermal unfolding, and thus does not end up in the same final state as obtained from chemical denaturation. This is consistent with the observation that thermally denatured HSA aggregates (Pico, 1995; Wetzel et al., 1980), whereas chemically denatured HSA does not. As the protein was cooled to 20°C, the anisotropy of the Trp residue returned to the initial value of 0.180 ± 0.002. However, the mean fluorescence lifetime (from Table 3) did not return to the value obtained for the native protein, resulting in a mean rotational correlation time of 3.71 ± 0.07 ns. Hence the mobility of the Trp residue was greater in the refolded state as compared to the native state. This clearly indicated that the protein did not refold to its original form after a single heating and cooling cycle.

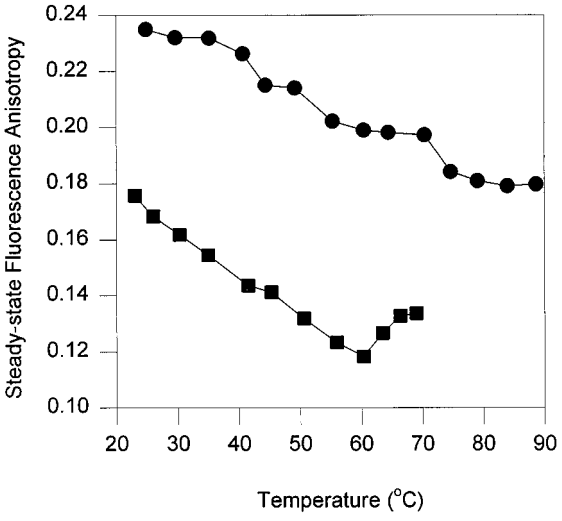

FIGURE 5 Steady-state fluorescence anisotropy of HSA and HSA-Ac during thermal denaturation. ■, Anisotropy of Trp from HSA with excitation at 295 nm. ●, Anisotropy of acrylodan within HSA-Ac with excitation at 360 nm.

Monitoring of Trp emission from HSA-Ac (*squares* in Fig. 4) provided evidence of two unfolding steps, in qualitative agreement with the multistep unfolding observed during chemical denaturation. In addition, the intensity of the Trp signal of HSA-Ac initially increased upon unfolding, consistent with an initial increase in the donor-acceptor distance with increasing temperature. With the exception of the two-step unfolding profile, the changes in Trp emission characteristics (intensity, wavelength, anisotropy) during unfolding were similar to those for unlabeled HSA.

Monitoring of acrylodan fluorescence (*triangles* in Fig. 4) also showed an initial increase in acrylodan intensity between 20°C and 30°C. Given that energy transfer is not possible under these experimental conditions, the spectroscopic changes provide evidence of a global change in protein structure that affected the environment in the region of both the Trp and the acrylodan label. Hence the initial structural changes involving domain separation must also have a direct effect on the environment surrounding Trp^{214} and Cys^{34}. Salicylate binding studies done at 40°C showed retention of partial binding function; hence complete domain separation was not evident at this point. Recovery of the temperature to 20°C resulted in almost full recovery of salicylate binding, suggesting that the initial changes in structure were reversible, in agreement with the chemical denaturation studies.

Between 30°C and 60°C, the acrylodan intensity varies somewhat, whereas the emission maximum blue shifts from 495 nm to 490 nm. The steady-state fluorescence anisotropy of the acrylodan label (Fig. 5, *circles*) also showed a significant decrease, corresponding reasonably well to the pretransition region (30–50°C). This clearly shows that the unfolding of domain II has a major effect on the environment of the acrylodan probe in domain I. Between 60°C and 90°C, the intensity and anisotropy of the acrylodan label decreased substantially, indicating the main unfolding transition of domain I. Over this range, the emission maximum of the acrylodan label blue shifted to 480 nm, indicating a decrease in the polarity in the local region of Cys^{34}. It is interesting to note that the emission maximum of the acrylodan label red shifted during chemically induced unfolding, which is opposite the trend observed during thermal denaturation. This suggests that domain I was able to fully unfold upon exposure to GdHCl, but could not unfold at high temperature. This is further supported by the final anisotropy value of 0.180 at 90°C, which is substantially higher that that for acrylodan in solution ($r_{acrylodan} = 0.005$), indicating that the protein was not fully unfolded at this temperature. The data are consistent with aggregation of the protein at higher temperatures. Salicylate binding studies of protein that was recovered from heating at 80°C indicated a

TABLE 3 Fluorescence intensity decay parameters for the Trp residue within HSA and the acrylodan moiety of HSA-Ac as a function of temperature

Sample	α_1	α_2	α_3	f_1*	f_2	f_3	τ_1 (ns)	τ_2 (ns)	τ_3 (ns)	$\langle\tau\rangle$ (ns)#	χ^2
Tryptophan in HSA											
20°C	0.57	0.29	0.14	0.79	0.20	0.01	5.913	3.046	0.231	5.28	1.054
75°C	0.38	0.62	—	0.67	0.33	—	3.251	0.984	—	2.50	1.030
20°C (recovered)	0.42	0.33	0.25	0.77	0.21	0.02	5.628	1.920	0.195	4.72	1.033
Acrylodan in HSA-Ac											
20°C	0.56	0.44	—	0.87	0.13	—	4.137	1.363	—	3.77	1.083
80°C	0.54	0.46	—	0.79	0.21	—	3.327	1.195	—	2.88	1.005
20°C (recovered)	0.64	0.36	—	0.85	0.15	—	4.046	1.269	—	3.62	1.022

*Calculated from Eq. 3.
#Calculated from Eq. 4.

large loss of binding function, confirming that the recovered protein was only partially functional.

The thermal melting curves derived from measurements of Trp intensity in HSA and HSA-Ac were examined using Eq. 10. The thermodynamic parameters for HSA indicated an enthalpy of unfolding of 350 ± 23 kJ · mol^{-1}, an entropy of unfolding of 1050 ± 71 J · K^{-1} · mol^{-1}, and a T_{un} value of 60 ± 4°C (note: other fitting parameters were as follows: F_{0N} = 1.251, F_{0U} = 0.850, s_N = −0.009, s_U = −0.006). These values are in excellent agreement with literature values (Pico, 1995, 1996, 1997). The ΔG_{un} value was determined to be 42 kJ · mol^{-1} if the $\Delta C_{p,un}$ value was set to zero. Use of the $\Delta C_{p,un}$ values provided by Pico (1997) resulted in negative free energy values at a reference temperature of 20°C, suggesting that these values may be erroneous. Thus all ΔG_{un} values reported herein use a $\Delta C_{p,un}$ value of zero. Thermodynamic analysis of the first unfolding step for HSA-Ac yielded thermophysical values that were similar to those obtained for unlabeled, native HSA (ΔH_{un} = 380 ± 25 kJ · mol^{-1}, ΔS_{un} = 1160 ± 60 J · K^{-1} mol^{-1}, ΔG_{un} = 39.6 ± 6.7 kJ · mol^{-1}, F_{0N} = 1.142, F_{0U} = 1.012, s_N = −0.006, s_U = −0.007). From these values, the unfolding temperature was calculated to be 55 ± 3°C, which is in reasonable agreement with the value obtained for unlabeled, native HSA. The small differences in the T_{un} values likely reflect the influence of the acrylodan label on the emission properties of Trp within HSA-Ac, because of energy transfer. Circular dichroism spectra of HSA-Ac obtained in 10 mM phosphate buffer containing 100 mM KCl, pH 7.2, suggested that the labeled protein was 64% α-helix, 21% β-sheet, and 15% random coil (data not shown). These values are in excellent agreement with those obtained by Wetzel et al. (1980) for native HSA under similar conditions (61% α-helix, 22% β-sheet, 17% random coil). These results indicate that labeling of Cys^{34} had no significant effect on the conformation of the native protein, ruling out such changes as the basis of the lower T_{un} for HSA-Ac.

The unfolding curve derived from measurements of acrylodan fluorescence intensity could not be fit to Eq. 10, because there was no postunfolding region, owing to the inability of our instrument to heat samples beyond 92°C. However, qualitative analysis of the unfolding curve suggests that the T_{un} is at least 75°C. It must be noted that the determination of thermodynamic parameters relies on the protein unfolding being reversible. The spectroscopic parameters strongly suggest that this is not a valid assumption for HSA; thus the thermodynamic data presented above should be treated with caution.

The time-resolved decay of fluorescence intensity was examined for the Trp residue of HSA and the acrylodan probe of HSA-Ac at different temperatures and upon recovery from 75°C (for HSA) or 80°C (for HSA-Ac). The results are given in Table 3. Unfolding of the protein by raising the temperature to 75°C resulted in the decay being best fit by two decay components and caused a decrease in the intensity-weighted mean fluorescence lifetime from 5.28 ± 0.03 ns to a value of 2.50 ± 0.05 ns. Refolding the protein by decreasing the temperature to 20°C resulted in the reappearance of the third decay component; however, the lifetime recovered to only 4.72 ± 0.09 ns. In addition, the fractional contributions of each decay component were different from those observed for the native protein, with the fraction of the shortest component increasing at the expense of the longest component. This clearly indicated that the native protein structure was not fully recovered upon protein refolding, at least in the region of the Trp residue, in agreement with the chemical denaturation studies described above. Previous studies of the unfolding and refolding behavior of HSA using circular dichroism measurements indicated that the α-helical content of the protein decreased upon thermal denaturation to 75°C and did not fully recover upon subsequent cooling (Wetzel et al., 1980). Thus the α-helix containing the Trp residue may have been altered to a looser structure similar to a random coil upon unfolding, and the new conformation was likely to be unable to refold into the original form. The fluorescence lifetime characteristics of the refolded state obtained after chemical denaturation were effectively identical to those measured for the protein after recovery from thermal denaturation. This was not expected, because the spectra of the two recovered proteins are quite different in terms of wavelength and intensity.

Table 3 also shows the preexponential terms and fluorescence lifetime components obtained for the acrylodan probe within HSA-Ac at 20°C, after heating to 80°C and after subsequent recovery to 20°C. These data clearly show that both lifetime components decrease upon heating; however, the shorter of the two components decreases by 63%, whereas the longer component drops by only 18%. Cooling to 20°C caused the mean lifetime to recover to within a few percent of the original value; however, there was once again a significant difference in the value and the contribution of the short lifetime component, indicating that the environment within the cybotactic region surrounding the acrylodan probe did not recover to the initial conditions before heating. These results are consistent with those for the Trp residue in HSA, and overall suggest that the protein does not refold to its native structure after heating beyond the protein T_{un}.

Time-resolved anisotropy provided evidence of increased rotational motion of the acrylodan probe upon heating of the protein, as shown in Fig. 6. The global reorientation time was again higher than expected (~55 ns), as was found during chemical denaturation studies, further supporting the presence of protein dimers or multimers. Interestingly, both the global and local rotational correlation times decreased substantially over the first 10°C increase (20°C to 30°C). This corresponds to the temperature range for the initial increase observed in the intensity of the acrylodan label and the increase in the Trp signal when HSA-Ac was denatured. This suggests that there may be a pretransition, or perhaps a local change in the environment of the acrylodan label (domain separation). However, there appear to be no corresponding changes in steady-state anisotropy. Further increases in temperature up to 90°C caused the global correlation time to decrease until a temperature of 70°C was reached, at which point a slight increase in ϕ_2 was observed. The most striking change in the time-resolved fluorescence anisotropy was the significant increase in the contribution from the local rotational motion, as evidenced by the large increase in β_1 between 60°C and 80°C, which corresponds well to the region where the acrylodan intensity reported the unfolding of domain I.

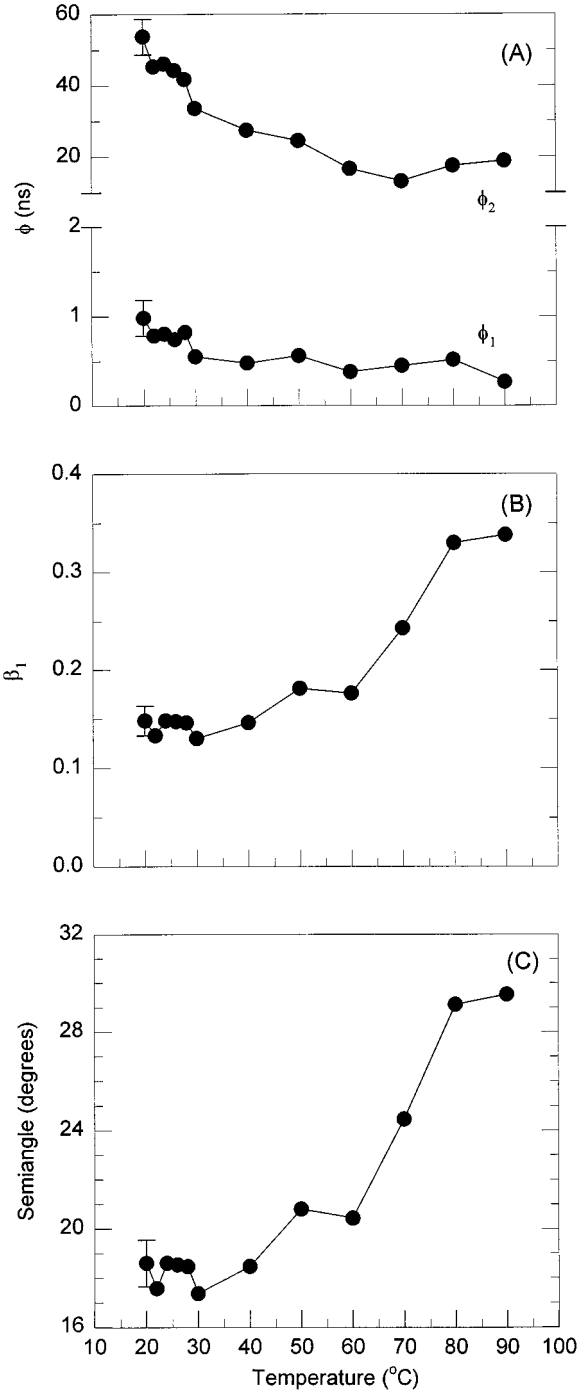

FIGURE 6 Time-resolved anisotropy of acrylodan within HSA-Ac during thermal denaturation. (*A*) Fluorescence rotational correlation times for global (ϕ_2) and local (ϕ_1) rotational components. (*B*) Fractional contribution of ϕ_1 as a function of temperature. (*C*) Semiangle of probe rotation obtained during heating of the protein. The error bars on each panel denote ±1 standard deviation from at least three discrete measurements.

A model for unfolding of HSA

Based on the results presented above, the following model for unfolding of HSA can be developed. Based on salicylate binding studies, it is clear that raising the temperature to <50°C or adding up to 1.0 M of GdHCl causes a complete loss of protein function, but that this process is almost fully reversible. Energy transfer results suggest that domains I and II move apart during this stage, causing slight alterations in the local environments of both the Trp and acrylodan residue. This conclusion is based on the observed changes in emission maximum values for both probes, the increase in Trp intensity over this range for HSA-Ac (Fig. 2 *B*), and the slight changes in the time-resolved decay of intensity and anisotropy for the acrylodan moiety. Increasing the temperature above 60°C or increasing the level of denaturant to 2.0 M resulted in substantial changes in the spectroscopic parameters for the Trp residue. Both the integrated intensity and the steady-state anisotropy of the Trp

residue drop significantly over this range. In the case of chemical denaturation, this change was accompanied by a 15-nm red shift in the emission maximum, a doubling of the k_q value, and a decrease of 16% in the mean fluorescence lifetime. For thermal unfolding, the emission maximum did not shift significantly. However, the fluorescence lifetime dropped by 53%. Together, these changes indicate a major structural change for the protein which is consistent with the unfolding of domain II. The spectroscopic parameters for the acrylodan probe over this temperature or denaturant range changed only slightly, with most parameters changing value by only a few percent. The most notable changes for acrylodan were the slight decrease in semiangle, which was accompanied by a 5-nm blue shift in the emission maximum for the probe. These changes are consistent with a slight closing of the pocket surrounding the acrylodan moiety, and may be indicative of an indirect effect of domain II unfolding on the environment of domain I. Salicylate binding studies indicated that this stage of unfolding was only partially reversible, in agreement with the altered spectroscopic parameters for the Trp residue for the recovered protein.

Increasing the temperature above 70°C or higher, or the level of GdHCl to 4.0 M or above, resulted in small changes in the spectroscopic behavior of the Trp residue, but had a significant effect on the emission properties of the acrylodan moiety. For example, the integrated intensity and anisotropy both decreased substantially between 2.2 M and 5.0 M GdHCl, with corresponding decreases in the mean fluorescence lifetime. For chemical denaturation, a 10-nm red shift in the emission maximum and a 70% increase in the k_q value of the acrylodan moiety were also observed, with the semiangle for acrylodan rotation increasing by 9°. Overall, these changes indicate that the acrylodan moiety becomes much more solvent exposed and more mobile, consistent with the unfolding of domain I. In addition, the energy transfer experiment indicated a significant increase in the average Trp-to-acrylodan distance, providing further evidence of an overall expansion in the size of the protein. Salicylate binding experiments indicated that these structural alterations were only partially reversible. Thus the unfolding of either domain I or domain II causes a significant loss in protein function.

The denaturation experiments indicate that the unfolding of HSA proceeds by the following scheme:

$$N \overset{\text{Step 1}}{\longleftrightarrow} E \overset{\text{Step 2}}{\longrightarrow} I \overset{\text{Step 3}}{\longrightarrow} U \qquad \text{(I)}$$

where N is the native form of the protein, E is the expanded form, I is an intermediate where domain II is unfolded but domain I is intact, and U is the unfolded protein. The scheme proposed above is consistent with previous reports, which show that heating HSA to temperatures less than 60°C results in refolding being fully reversible, whereas heating to higher temperatures results in a substantial loss of reversibility for the unfolding transition (Pico, 1997). This model is also consistent with previous reports that suggest a multistep unfolding pathway for HSA (Wallevick, 1973; Chmelik and Kalous, 1982; Pico, 1997). However, our model is the first to provide detailed insight into the nature of the various unfolding intermediates, and is the first to show that unfolding of domain I occurs only after the unfolding of domain II is complete. Spectroscopic data from both the Trp and acrylodan probes suggest that the *U* state shown in Scheme I is not a fully unfolded random coil, but rather a partially unfolded or molten globule state. This is likely the result of intact disulfide bonds within the various domains, which act to maintain a degree of structure (Lee and Hirose, 1992). The addition of a disulfide reducing agent was not attempted, because this would have removed the acrylodan label from Cys^{34}.

JDB thanks the Natural Sciences and Engineering Research Council of Canada, and FVB thanks the National Science Foundation (grant no. CHE-9300694) for financial support of this work. We also thank Prof. Arthur G. Szabo of the University of Windsor for providing access to fluorescence lifetime equipment.

REFERENCES

Brown, J. R. 1977. Serum albumin: amino acid sequence. *In* Albumin Structure, Function and Uses. V. M. Rosenoer, M. Oratz, and M. A. Rothschild, editors. Pergamon, Oxford. 27–51.

Brown, K. F., and M. J. Crooks. 1976. Displacement of tolbutamide, glibenclamide and chlorpropamide from serum albumin by anionic drugs. *Biochem. Pharmacol.* 25:1175–1178.

Campbell, I. D., and R. A. Dwek. 1984. Biological Spectroscopy. Benjamin/Cummings, London.

Carter, D. C., and J. X. Ho. 1994. Structure of serum albumin. *Adv. Protein Chem.* 45:153–203.

Chmelik, J., and V. Kalous. 1982. Polarographic investigation of conformational changes of human serum albumin. Part I. Unfolding of human serum albumin by urea. *Bioelectrochem. Bioenerg.* 9:7–13.

Clark, I. D., and L. D. Burtnick. 1988. Fluorescence of equine platelet tropomyosin labeled with acrylodan. *Arch. Biochem. Biophys.* 260: 595–600.

Edmiston, P. L., C. L. Wambolt, M. K. Smith, and S. S. Saavedra. 1994. Spectroscopic characterization of albumin and myoglobin entrapped in bulk sol-gel glasses. *J. Colloid Interface Sci.* 163:395–406.

Eftink, M. R. 1994. The use of fluorescence methods to monitor unfolding transitions in proteins. *Biophys. J.* 66:482–501.

Eftink, M. R., and C. A. Ghiron. 1976. Exposure of tryptophyl residues in proteins. Quantitative determination by fluorescence quenching studies. *Biochemistry.* 15:672–679.

Farruggia, B., G. Gabriela, C. D'Angelo, and G. Pico. 1997. Destabilization of human serum albumin by polyethylene glycols studied by thermodynamical equilibrium and kinetic approaches. *Int. J. Macromol.* 20:43–51.

Hagag, N., E. R. Birnbaum, and D. W. Darnall. 1983. Resonance energy transfer between cysteine-34, tryptophan-214, and tyrosine-411 of human serum albumin. *Biochemistry.* 22:2420–2427.

Helms, M. K., C. E. Petersen, N. V. Bhagavan, and D. M. Jameson. 1997. Time-resolved fluorescence studies on site-directed mutants of human serum albumin. *FEBS Lett.* 408:67–70.

Hultmark, D., K. Borg, R. Elofsson, and L. Palmer. 1975. Interaction between salicylic acid and indometacin in binding to human serum albumin. *Acta Pharm. Suec.* 12:259–276.

Ilich, P., and F. G. Prendergast. 1989. Singlet adiabatic states of solvated prodan: a semi-empirical molecular orbital study. *J. Phys. Chem.* 93: 4441–4447.

Ingersoll, C. M., J. D. Jordon, and F. V. Bright. 1996. Accessibility of the fluorescent reporter group in native, silica-adsorbed, and covalently attached acrylodan-labeled serum albumins. *Anal. Chem.* 68: 3194–3198.

Jordon, J. D., R. A. Dunbar, and F. V. Bright. 1995. Dynamics of acrylodan-labeled bovine and human serum albumin entrapped in a sol-gel-derived biogel. *Anal. Chem.* 67:2436–2443.

Kerestes-Nagy, S., R. F. Mais, Y. T. Dester, and J. F. Zaroslinski. 1972. Comparison of equilibrium dialysis and frontal analysis chromatography in the study of salicylate binding. *Anal. Biochem.* 48:80–89.

Lakowicz, J. R., and G. Weber. 1973. Quenching of fluorescence by oxygen. A probe for structural fluctuations in macromolecules. *Biochemistry.* 12:4161–4170.

Lee, J. Y., and M. Hirose. 1992. Partially folded state of the disulfide-reduced form of human serum albumin as an intermediate for reversible denaturation. *J. Biol. Chem.* 267:14753–14758.

Lundgren, J. S., M. P. Heitz, and F. V. Bright. 1995. Dynamics of acrylodan-labeled bovine and human serum albumin sequestered with aerosol-OT reverse micelles. *Anal. Chem.* 67:3775–3781.

Narazaki, R., T. Maruyama, and M. Otagiri. 1997. Probing the cysteine 34 residue in human serum albumin using fluorescence techniques. *Biochim. Biophys. Acta.* 1338:275–281.

O'Connor, D. V., and D. Phillips. 1984. Time-Correlated Single Photon Counting. Academic Press, London.

Pico, G. A. 1995. Thermodynamic aspects of the thermal stability of human serum albumin. *Biochem. Mol. Biol. Int.* 36:1017–1023.

Pico, G. A. 1996. Thermal stability of human serum albumin by sodium halide salts. *Biochem. Mol. Biol. Int.* 38:1–6.

Pico, G. A. 1997. Thermodynamic features of the thermal unfolding of human serum albumin. *Int. J. Biol. Macromol.* 20:63–73.

Prendergast, F. G., M. Meyer, G. L. Carlson, S. Iida, and J. D. Potter. 1983. Synthesis, spectral properties, and use of 6-acryloyl-2-dimethylaminonaphthalene (acrylodan). *J. Biol. Chem.* 258:7541–7544.

Price, W. S., N.-H. Ge, L.-Z. Hong, and L.-P. Hwang. 1993. Characterization of chloride ion binding to human serum albumin using CI-NMR null point spectral analysis. *J. Am. Chem. Soc.* 115:1095–1105.

Santoro, M. M., and D. W. Bolen. 1988. Unfolding free energy changes determined by the linear extrapolation method. 1. Unfolding of phenylmethanesulfonyl α-chymotrypsin using different denaturants. *Biochemistry.* 27:8063–8068.

Sudlow, G., D. J. Birkett, and D. N. Wade. 1976. Further characterization of specific drug binding sites on human serum albumin. *Mol. Pharmacol.* 12:1052–1061.

Suzukida, M., H. P. Le, F. Shahid, R. A. McPherson, E. R. Birnbaum, and D. W. Darnall. 1983. Resonance energy transfer between cysteine-34 and tryptophan-214 in human serum albumin. Distance measurements as a function of pH. *Biochemistry.* 22:2415–2420.

Tayyab, S., M. U. Siddiqui, and N. Ahmad. 1995. Experimental determination of the free energy of unfolding of proteins. *Biochem. Ed.* 23: 162–164.

Wallevick, K. 1973. Reversible denaturation of human serum albumin by pH, temperature, and guanidine hydrochloride followed by optical rotation. *J. Biol. Chem.* 248:2650–2655.

Wang, R., and F. V. Bright. 1993. Rotational reorientation kinetics of dansylated bovine serum albumin. *J. Phys. Chem.* 97:4231–4238.

Wang, R., S. Sun, E. J. Bekos, and F. V. Bright. 1996. Dynamics surrounding Cys-34 in native, chemically denatured, and silica-adsorbed bovine serum albumin. *Anal. Chem.* 67:149–159.

Wetzel, R., M. Becker, J. Behlke, H. Wite, S. Bohn, B. Ebert, H. Hamaann, J. Krumbiegel, and G. Lasiman. 1980. Temperature behaviour of human serum albumin. *Eur. J. Biochem.* 104:469–478.

Yem, A. W., D. E. Epps, W. R. Matthews, D. M. Guido, K. A. Richard, N. D. Staite, and M. R. Deibel, Jr. 1992. Site-specific chemical modification of interleukin-1β by acrylodan at cysteine 8 and lysine 103. *J. Biol. Chem.* 267:3122–3128.

Zheng, L., W. R. Reid, and J. D. Brennan. 1997. Measurement of fluorescence from tryptophan to probe the environment and reaction kinetics within protein-doped sol-gel-derived glass monoliths. *Anal. Chem.* 69: 3940–3949.